THE JOURNAL OF BIOLOGICAL CHEMISTRY
Vol. 278, No. 46, Issue of November 14, pp. 46146–46154, 2003
Printed in U.S.A.

Energetics of the Cooperative Assembly of Cell Division Protein FtsZ and the Nucleotide Hydrolysis Switch*

Received for publication, July 3, 2003, and in revised form, August 6, 2003
Published, JBC Papers in Press, August 21, 2003, DOI 10.1074/jbc.M307128200

Sonia Huecas‡ and José Manuel Andreu‡

From the Centro de Investigaciones Biológicas, CSIC, Ramiro de Maeztu 9, E-28040 Madrid, Spain

FtsZ is the first protein recruited to the bacterial division site, where it forms the cytokinetic Z ring. We have determined the functional energetics of FtsZ assembly, employing FtsZ from the thermophilic Archaea *Methanococcus jannaschii* bound to GTP, GMPCPP, GDP, or GMPCP, under different solution conditions. FtsZ oligomerizes in a magnesium-insensitive manner. FtsZ cooperatively assembles with magnesium and GTP or GMPCPP into large polymers, following a nucleated condensation polymerization mechanism, under nucleotide hydrolyzing and non-hydrolyzing conditions. The effect of temperature on the critical concentration indicates polymer elongation with an apparent heat capacity change of −800 ± 100 cal mol^{-1} K^{-1} and positive enthalpy and entropy changes, compatible with axial hydrophobic contacts of each FtsZ in the polymer, and predicts optimal polymer stability near 75 °C. Assembly entails the binding of one medium affinity magnesium ion and the uptake of one proton per FtsZ. Interestingly, GDP- or GMPCP-liganded FtsZ cooperatively form helically curved polymers, with an elongation only 1–2 kcal mol^{-1} more unfavorable than the straight polymers formed with nucleotide triphosphate, suggesting a physiological requirement for FtsZ polymerization inhibitors. This GTP hydrolysis switch should provide the basic properties for FtsZ polymer disassembly and its functional dynamics.

Both prokaryotic and eukaryotic cells use dynamic protein assemblies to fulfill central roles in DNA segregation, cell division, cell shape, and polarity (1–3). Several of these are cytoskeletal assemblies made of nucleotide-binding proteins, which share homologous frameworks, indicating that they have evolved from common ancestors. Thus tubulin (4), the main component of the microtubules of the mitotic spindle that segregates chromosomes, and FtsZ (5), which forms the Z-ring directing bacterial cell division, share the same fold in two of their domains and constitute a distinct family of assembling GTPases (6). Actin (7), which assembles into microfilaments, is a homologue of MreB (8), which assembles into similar filaments determining bacterial cell shape. Other prokaryotic members of the actin family of ATP-binding proteins include ParM, which assembles into actin-like filaments responsible for plasmid segregation (9), and FtsA, which is thought to anchor FtsZ to the membrane and recruit downstream cell division proteins (10).

To understand how each of the bacterial protein machines works (11, 12), in addition to their *in vivo* partner proteins, their structures and those of their polymers, a better knowledge is required of the functional energetics, the kinetics and mechanism of their assembly, and of how these may be modulated in the cytosolic environment. FtsZ, the homologue of eukaryotic tubulin, is ubiquitous in Eubacteria, Archaea, and chloroplast. Green fluorescent protein-fused FtsZ has a rapid assembly dynamics in the bacterial Z-ring, comparable to tubulin in a mitotic spindle (13, 14). Purified FtsZ forms a number of different polymers depending on the conditions (15–23). Monomers of FtsZ from *E. coli* form oligomers, in a magnesium-induced indefinite linear self-association equilibrium, with a light gradual decrease of the affinity of monomer addition with the oligomer size; replacement of GDP by GTP did not increase the affinity of this self-association (24). Lowering the pH and increasing the temperature triggered a different reaction, consisting in the GTP and magnesium-induced assembly[1] of large bi-dimensional polymers made of many FtsZ monomers; it was proposed that the linear oligomers correspond to primary steps for assembly (24). The energetics of assembly of FtsZ has not been characterized before. Apparently contradictory reports have either indicated (16, 19, 22) or questioned (23) whether the polymerization of FtsZ and the induction of the GTPase are cooperative. Archaeal FtsZ from *M. jannaschii* is activated for assembly by GTP binding, which has been predicted by molecular dynamics to change the conformation of switch loop T3 at the longitudinal assembly interface (25). This archaeal FtsZ reversibly assembles into polymers, whose filaments are made of two symmetrical tubulin-like protofilaments, which hydrolyze GTP and disassemble upon nucleotide consumption (26). In this work we have addressed the assembly equilibrium of archaeal FtsZ with GTP, GMPCPP,[2] GDP, and GMPCP nucleotides. The results clearly establish that FtsZ assembles in a cooperative condensation polymerization reaction, consistent with the double-stranded filament formation (26). Its modulation by temperature and solution variables has been character-

* This work was supported in part by MCyT Grants BIO99-0859-C03-02/BIO2002-03665, CAM Programa de Grupos Estratégicos, and Red Temática de Investigación Cooperativa FIS C03/14. This work was presented at a Workshop on Bacterial Cell Division (71), Juan March Centre for International Meetings on Biology (2002) Vol. 146, p. 72, Madrid. The costs of publication of this article were defrayed in part by the payment of page charges. This article must therefore be hereby marked "*advertisement*" in accordance with 18 U.S.C. Section 1734 solely to indicate this fact.

‡ To whom correspondence should be addressed. Fax: 34-91-5360432; E-mail: sonia@cib.csic.es or j.m.andreu@cib.csic.es.

[1] By self-association we mean the formation of oligomers or quaternary structure, whereas macromolecular assembly distinctly refers to the formation of large polymers and biological superstructures (72). These definitions intend to clarify some confusing citation of our previous work describing the quasi-isodesmic self-association of FtsZ (24) in the context of a so-called isodesmic assembly mechanism (23, 48), and the wrong recollection that analysis of the analytical ultracentrifugation data suggests the presence of long straight filaments (73).

[2] The abbreviations used are: GMPCPP, guanosine 5′-(α,β-methyleneotriphosphate); Mes, 4-morpholineethanesulfonic acid; HPLC, high performance liquid chromatography; CD, circular dichroism; PIPES, 1,4-piperazinediethanesulfonic acid.

ized and compared with tubulin assembly. It has been found that the GTP/GDP hydrolysis switch entails, instead of disassembly, a helical curvature of FtsZ filaments with a small free energy difference for polymer growth.

EXPERIMENTAL PROCEDURES

FtsZ Protein Expression and Purification—FtsZ from *M. jannaschii* without a Gly-Ser-His_6 C-terminal extension was overproduced in *Escherichia coli* BL21(DE3) pLys, and it was purified by ammonium sulfate precipitation, ion-exchange, and hydrophobic chromatography (26), stored at −80 °C in 20 mM Tris (pH 8.0), 1 mM EDTA, 1 mM NaN_3. FtsZ was equilibrated in the desired buffer by chromatography on Sephadex G-25 prior to use. Protein concentrations were measured from UV absorption spectra in 6 M guanidinium chloride, after subtracting the contribution of the bound guanosine nucleotide, and also approximately measured from native spectra (27). Purified FtsZ from *M. jannaschii* contained 0.45 ± 0.05 nucleotide bound (of which 79 ± 8% was GTP and 21 ± 8% was GDP), which increased to 0.92 ± 0.04 nucleotide upon equilibration with 10 μM GDP or GMPCPP.

Nucleotides, Nucleotide Extraction, and Analysis—GTP, dilithium salt, was from Roche Diagnostics. GDP, sodium salt was from Sigma (type I) and contained −1.5% GTP. GMPCPP and GMPCP were from Jena Biosciences. Nucleotides were extracted from FtsZ solutions by the method of Seckler *et al.* (28) with minor modifications. After addition of ice-cold $HClO_4$ to a final concentration of 0.5 M, the solution was incubated on ice for 10 min and denatured protein was removed by centrifugation (10 min, 10,000 × *g*, 4 °C). The supernatant was neutralized and buffered by the addition of one-sixth volume of 1 M K_2HPO_4, one-sixth volume of 3 M KOH and made 0.5 M acetic acid. Upon mixing, samples were frozen at −20 °C until HPLC analysis. Nucleotides were separated by isocratic reversed-phase ion-pair HPLC (29) on octadecyl silica (Supelco LC-18-DB 25 cm × 4.6 mm) and detected by their absorbance at 254 nm. The composition of the mobile phase was 0.2 M K_2HPO_4, 0.1 M acetic acid plus 4 mM tetrabutylammonium phosphate. The injection volume was 20 μl, and the flow rate was 1 ml/min.

Analytical Centrifugation and Circular Dichroism—Sedimentation equilibrium and velocity measurements were performed at 20 and 38 °C in an Optima XL-A (Beckman-Coulter) analytical ultracentrifuge as described (24). Whole cell apparent average molecular weights of FtsZ were obtained using the program EQASSOC (30). Sedimentation coefficients were calculated by global fitting of multiple sedimentation profiles with the program SVEDBERG (retrieved from the RASMB server (31).

The far-UV circular dichroism spectra of FtsZ (5–50 μM) were acquired with JASCO J720 and J810 dicrographs, using 0.1- and 0.01-cm cells in thermostated cell holders; the sample temperature was measured with a thermocouple.

FtsZ Assembly Characterization by Electron Microscopy and Light Scattering—M. jannaschii FtsZ was placed into a fluorometer cuvette thermostated to the desired temperature, and its 350-nm light scattering at a 90° angle was monitored with a Shimadzu RF 540 spectrofluorometer. FtsZ assembly was initiated by the addition of magnesium and the nucleotide to the cuvette. FtsZ samples were adsorbed to carbon-coated grids on a plate at the experimental temperature, negatively stained with 2% uranyl acetate, and observed under Jeol 1230 electron microscopes.

FtsZ Assembly Measurements by Sedimentation—FtsZ was equilibrated into potassium-containing Mes assembly buffer (50 mM Mes-KOH, 50 mM KCl, 1 mM EDTA, pH 6.5 or pH 6.0), or sodium-containing Mes assembly buffer (50 mM Mes-NaOH, 50 mM NaCl, 1 mM EDTA, pH 6.5 or 6.0). Reaction mixtures were prepared for a final volume of 100 μl in Beckman polycarbonate centrifuge tubes and incubated at the desired temperature (standard, 55 ± 1 °C) in a drilled aluminum block fitted to an Eppendorf Thermostat Plus. Assembly was started by adding magnesium and nucleotide. Unless indicated, the experiments were performed with 10 mM $MgCl_2$. GTP or GDP were added to a final concentration of 1 mM, GMPCPP or GMPCP to 0.1 mM. Samples were immediately placed into a prewarmed Beckman TL100 rotor and centrifuged 1.5–2 min later at 60,000 rpm for 6 min to pellet the FtsZ polymers. This procedure was found to give maximal polymer recovery with GTP under standard conditions and was readjusted when necessary by incubating the samples before centrifugation. For temperatures above 40 °C, the rotor was prewarmed 1 to 2 °C above the desired experimental temperature in an incubator, and the Beckman Optima TLX ultracentrifuge was set to 40 °C (the maximal setting allowed). This resulted in sample temperatures 1 to 2 °C above the desired value prior to centrifugation, and 1–2 °C below it just after the short centrifugation (measured with a small thermocouple). No more than six reactions were simultaneously sedimented to reduce the handling time. The supernatant was carefully withdrawn, the pellet was resuspended in the same volume of buffer, and their protein concentrations were measured (32) with the Bio-Rad protein assay kit in multiwell plates, employing spectrophotometrically calibrated FtsZ standards and a Titertek Multiskan MC plate reader with a 595-nm filter. Each protein concentration was tested at least twice per experiment and the results averaged.

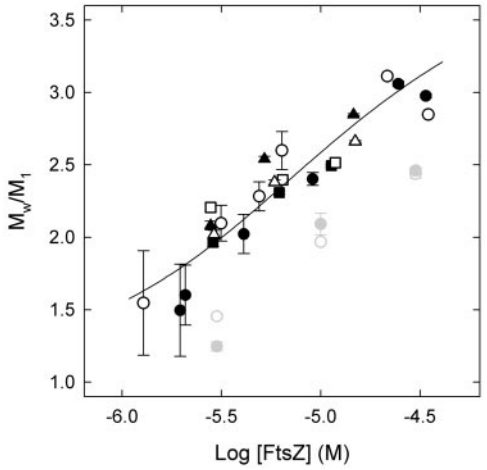

FIG. 1. **Analysis of the oligomerization of FtsZ by analytical ultracentrifugation in 50 mM Mes, 50 mM KCl, 50 μM EDTA, pH 6.5, at 20 °C.** The ratio of the weight average molecular mass to that of the FtsZ monomer is plotted *versus* FtsZ concentration. Each symbol type represents samples with a different nucleotides or nucleotide concentration: *circles* (●, ○), 50 μM GDP; *squares* (■, □), 10 μM GDP; *triangles* (▲, △), 10 μM GMPCPP. *Empty symbols* represent no magnesium addition and *solid symbols* represent the addition of 6 mM $MgCl_2$. The *solid line* is a best fit to a monomer-dimer-tetramer equilibrium model with association constants $K_{(\text{monomer} \rightleftarrows \text{dimer})} = 2.5 \times 10^5\ \text{M}^{-1}$ and $K_{(\text{dimer} \rightleftarrows \text{tetramer})} = 9.7 \times 10^9\ \text{M}^{-1}$. Association data in 50 mM Tris, 200 mM KCl, pH 8.0 without magnesium (*empty gray circles*) and with 6 mM $MgCl_2$ (*solid gray circles*) are also plotted for comparison (these points were not used for the model fit).

The elongation equilibrium constant (K_p) data (see "Results") at varying temperature were fitted by a nonlinear integrated van't Hoff equation (33) with Sigmaplot (Jandel Scientific) as shown in Equation 1,

$$\ln K_p = a + b(1/T) + c \ln T \quad \text{(Eq. 1)}$$

from which the apparent values of the free energy ΔG^0, enthalpy ΔH^0, entropy ΔS^0, and the heat capacity change ΔC_p, of the elongation reaction were calculated by Equations 2–5, respectively.

$$\Delta G^0 = -RT \ln(K_p) \quad \text{(Eq. 2)}$$

$$\Delta H^0 = R(cT - b) \quad \text{(Eq. 3)}$$

$$\Delta S^0 = (\Delta H^0 - \Delta G^0)/T \quad \text{(Eq. 4)}$$

$$\Delta C_p = Rc \quad \text{(Eq. 5)}$$

In experiments at varying magnesium concentration, the free Mg^{2+} concentrations were calculated from the total Mg^{2+} concentrations by solving the multiple equilibria, which take into account cation binding by EDTA and nucleotide as described (34).

RESULTS

Oligomerization of FtsZ from M. jannaschii Is Insensitive to Magnesium and Nucleotide—The association state of FtsZ was first studied using analytical ultracentrifugation. The apparent average molecular weight was measured by sedimentation equilibrium under different solution conditions and with different nucleotides (Fig. 1). Only at low enough concentrations (1–2 μM) FtsZ was close to monomer (M_r 38924), and the degree of FtsZ self-association increased with protein concentration in 50 mM Mes-KOH, 50 mM KCl, 50 μM EDTA buffer, pH 6.5. The association is compatible with the formation of a small FtsZ

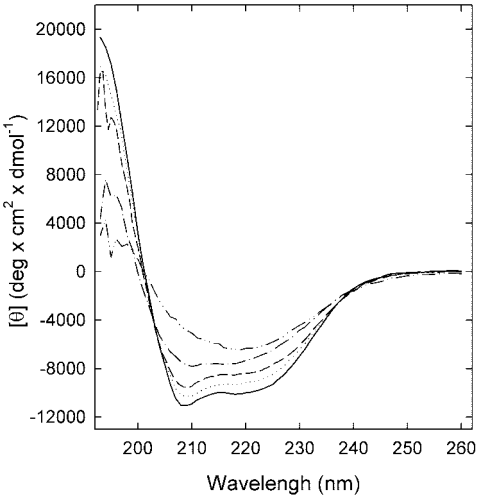

FIG. 2. **Variation of the far-UV CD spectrum of FtsZ (5 μM) as a function of temperature in 20 mM Tris-HCl, 0.1 mM EDTA, 50 μM GDP, pH 8.0.** Spectra were acquired at 25 °C (——), 55 °C (· · · · ·), 80 °C (- - - -), 95 °C (-·-·) and 100 °C (-··-··). A complete thermal denaturation profile could not be acquired under these conditions at atmospheric pressure. Similar results were obtained in potassium assembly buffer pH 6.5, except that the protein precipitated at 95–100 °C.

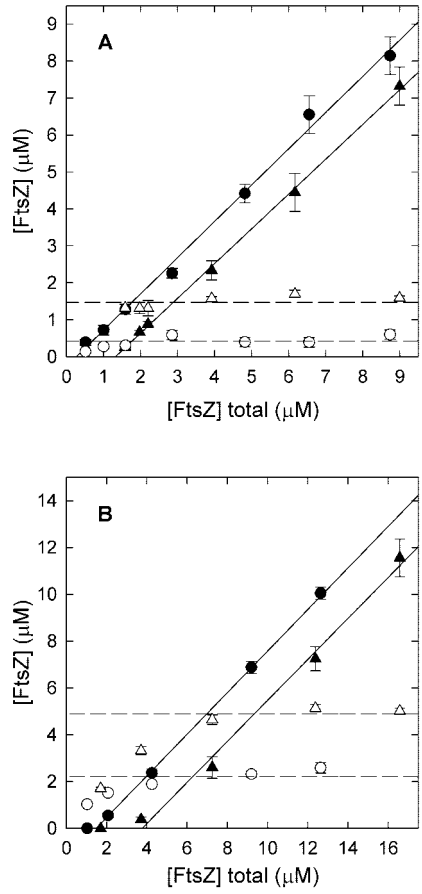

FIG. 3. **Sedimentation measurements of FtsZ polymers formed at 55 °C in (*panel A*) potassium-containing Mes assembly buffer, pH 6.5, 10 mM $MgCl_2$ and (*panel B*) sodium-containing Mes assembly buffer, pH 6.5, 10 mM $MgCl_2$.** FtsZ polymers were assembled with 0.1 mM GMPCPP or with 1 mM GTP. The symbols are: (●) GMPCPP pellet; (○) GMPCPP supernatant; (▲) GTP pellet; (△) GTP supernatant.

oligomer (up to a tetramer within the 1–40 μM FtsZ concentration range examined; see the model line in Fig. 1). No significant differences in the association behavior of FtsZ were found with Mg^{2+} (0 and 6 mM $MgCl_2$), or with the different nucleotides at the start of the experiments (10–50 μM GDP, 50 μM GTP, or 10 μM GMPCPP) at the temperatures employed (20 and 38 °C). The degree of association was slightly reduced in 50 mM Tris, 200 mM KCl, pH 8. The effects of nucleotides on the aggregation state of FtsZ were also examined by shorter sedimentation velocity measurements (in which GTP hydrolysis should be limited). The sedimentation coefficient of FtsZ at 20 °C had practically the same value ($s_{20,w}$ = 5.60 ± 0.13 S at 30 μM FtsZ) irrespectively of 10 μM GDP or 30 μM GTP nucleotide added and magnesium (0 or 6 mM $MgCl_2$). Since FtsZ easily exchanges its bound nucleotide under related conditions (25), we found no available evidence that the oligomerization of FtsZ from *M. jannaschii* is modulated by the nucleotide or by Mg^{2+} ions, at difference with the Mg^{2+}-induced self-association of bacterial FtsZ from *E. coli* (24).

Whether oligomerization, magnesium, nucleotides, pH, ionic strength, and temperature induced changes in the average secondary structure of FtsZ was examined by circular dichroism. The CD spectra of FtsZ showed no concentration dependence (5–50 μM FtsZ), and a lack of significant effects of $MgCl_2$ (0–10 mM), GDP or GMPCPP (10 μM), pH 6.5 or 8.0, and 0–500 mM KCl. The effects of temperature were very small between 25 and 80 °C, and at 95 and 100 °C a partial thermal unfolding of FtsZ could be evidenced by the loss of the α-helical CD minima at 208 and 222 nm (Fig. 2).

Cooperative Assembly of FtsZ—Raising the temperature with GTP or GMPCPP and Mg^{2+}, under otherwise the same conditions in which FtsZ forms small oligomers, resulted in the formation of large FtsZ polymers, which could be pelleted by differential centrifugation. Interestingly, these polymers formed above a given FtsZ critical concentration. Since FtsZ polymerization induces its GTPase activity (26), which leads to depolymerization, the polymer stability was also monitored by light scattering under the same experimental conditions. FtsZ was incubated in assembly buffer, magnesium, and the nucleotide (1 mM GTP or 0.1 mM GMPCPP) were added, and the samples centrifuged; the incubation and centrifugation times (see "Experimental Procedures") were adjusted for optimal recovery of pelletable polymer before disassembly by nucleotide consumption. The FtsZ concentrations from the pellet and in the supernatant were plotted against the initial concentration. Representative results are shown by Fig. 3, in which it can be appreciated that (i) FtsZ forms pelletable polymers only above a given critical total protein concentration and (ii) the slope of the polymerized *versus* total protein concentration plot is unitary, indicating that essentially all the protein excess above critical concentration had polymerized and had been efficiently sedimented.[3]

These results (Fig. 3*A*) show that FtsZ from *M. jannaschii* cooperatively polymerizes following a nucleated condensation mechanism, similarly to other fiber-forming protein polymerization processes (35–40). For such a cooperative assembly the apparent equilibrium constant (K_p) for the growth reaction (the addition of a monomer to the polymer) is in good approximation equal to the reciprocal critical concentration (36). The critical concentration for FtsZ assembly with 1 mM GTP and 10 mM $MgCl_2$ was 50.6 ± 4.3 μg/ml (1.3 ± 0.11 μM, Table I), resulting in $K_p = (7.7 \pm 0.7) \times 10^5\ M^{-1}$, and an apparent free energy change of polymer growth $\Delta G^0_{g,app} = -RT\ln(K_p) = -8.84 \pm 0.06$ kcal mol^{-1} (55 °C). With the slowly hydrolyzable analogue

[3] Typical values of the slope of the pellet *versus* total FtsZ concentration plot were 0.90–0.92, suggesting the presence of 8–10% of the protein incompetent to polymerize. This was confirmed by giving a cycle of polymerization to the protein before measurements, which resulted in slope values of 0.97 ± 0.02.

TABLE I
Effects of nucleotide on the critical concentration, and nucleotide content of FtsZ polymers, in potassium- and sodium-containing assembly buffers

Nucleotide employed	K^+/pH 6.5		K^+/pH 6.0	Na^+/pH 6.5		Na^+/pH 6.0
	Cr	Polymer bound nucleotide[a]	Cr	Cr	Polymer bound nucleotide[a]	Cr
	μM		μM	μM		μM
GMPCPP[b]	0.29 ± 0.08	25% GMPCPP (78%), 75% GMPCP (22%)	0.16 ± 0.02	1.47 ± 0.08	98% GMPCPP, 2% GMPCP	0.91 ± 0.30
GMPCP[c]	10.6 ± 1.40	80% GMPCP, 20% GMPCPP	4.20 ± 0.33	8.00 ± 1.02	85% GMPCP, 20% GMPCPP	3.55 ± 0.30
GTP[b]	1.30 ± 0.11	49% GTP (84%), 51% GDP (16%)	0.60 ± 0.09	4.00 ± 0.60	98% GTP, 2% GDP	1.77 ± 0.40
GDP[d]	17.50 ± 1.80	98% GDP, 2% GTP	12.50 ± 1.50	nd[e]	nd	8.73 ± 1.28

[a] The nucleotide which cosedimented with the polymer were extracted from the pellets and analyzed by HPLC: numbers in parenthesis are the corresponding values in the supernatant, which confirm an excess of GTP or GMPCPP.
[b] 0.1 mM GMPCPP or 1 mM GTP were added to the reaction mixture.
[c] FtsZ was previously assembled with GMPCPP which was let to hydrolyze, then equilibrated with 10 μM GMPCP and the reaction mixture was supplemented to 0.1 mM GMPCP (simple nucleotide addition was inefficient).
[d] FtsZ was previously equilibrated with 10 μM GDP and supplemented to 1 mM GDP (similar results were obtained by GDP addition).
[e] nd, not determined.

GMPCPP (0.1 mM) the critical concentration was lower than with GTP and therefore the propagation constant increased: Cr = 11.3 ± 3.3 μg/ml (0.29 ± 0.08 μM, Table I), K_p = (3.4 ± 0.1) × 10^6 M^{-1}, and $\Delta G^0_{g,app}$ = −9.82 ± 0.20 kcal mol^{-1}. This gives an advantage of $\Delta\Delta G^0_{g,app}$ (GMPCPP-GTP) = −1.04 ± 0.15 kcal mol^{-1} favorable to elongation with GMPCPP (corrected to the same free Mg^{2+} concentration; see below).

Since both GTP and GMPCPP are hydrolyzed during FtsZ assembly, and the kinetic mechanisms of assembly, nucleotide hydrolysis and exchange are essentially unknown, it can be argued that the system is not at equilibrium and that these apparent thermodynamic values may be somehow biased by the nucleotide hydrolysis. Therefore the same measurements were made in Na^+-containing assembly buffer pH 6.5, in which the GTPase activity of FtsZ is inhibited and stable polymers are formed (26). FtsZ assembly is slightly less favored with Na^+, however, due to the absence of nucleotide hydrolysis the system becomes a rigorous chemical equilibrium. The results of these measurements, shown by Fig. 3*B* and Table I, indicate ΔG^0_{app} (GTP) = −8.10 ± 0.10 kcal mol^{-1}, ΔG^0_{app} (GMPCPP) = −8.76 ± 0.04 kcal mol^{-1}, and $\Delta\Delta G^0_{app}$(GMPCPP-GTP) = −0.66 ± 0.08 kcal mol^{-1} favorable to elongation with GMPCPP, which confirms the result in K^+-buffer. The assembly elongation is enhanced in the K^+-buffer by $\Delta\Delta G^0_{app}$(K^+ minus Na^+) = −0.74 ± 0.07(GTP) or −1.06 ± 0.14 (GMPCPP) kcal mol^{-1}.

Analyzing the polymer-bound nucleotide when FtsZ was assembled with 0.1 mM GMPCPP or 1 mM GTP indicated that under non-hydrolyzing conditions in Na^+-containing buffer at pH 6.5, the nucleotide bound to the polymer was 98% GMPCPP or GTP, respectively (Table I). However, when FtsZ was assembled under hydrolyzing conditions in K^+-containing buffer, the bound nucleotide was only 25% GMPCPP (75% GMPCP) or 49% GTP (51% GDP), respectively (Table I). Since polymerizing FtsZ repeatedly hydrolyzes GTP from the solution, at a rate of several GTP per minute under closely related conditions (26), these results indicate that the nucleotide is exchanged by polymerizing FtsZ (that is, by the polymers or by rapidly exchanging monomers), possibly in a rate-limiting step comparable to the observed hydrolysis rate (otherwise the nucleotide in the polymer would be all GDP or all GTP). Since GTP hydrolysis continues during centrifugation but steady state exchange of fresh GTP from the solution may be hindered by entrapment in the pellet, these percent hydrolysis values may be regarded as maximal estimates of the true values in the FtsZ polymers prior to centrifugation.

The polymers formed by FtsZ under these conditions were characterized by electron microscopy (Fig. 4). FtsZ formed large filamentous polymers, which were 30–60 nm wide with GTP (Fig. 4*A*), and 80–120-nm wide with GMPCPP (Fig. 4*B*), and which were observed together with isolated filaments which correspond to the double stranded elementary assembly product of FtsZ from *M. jannaschii* (26). In the Na^+-containing buffer, the predominant polymers were roughly 8-nm wide isolated filaments (Fig. 4*C*). It is possible that the small energetic difference between elongation in both buffers may be related to the more extensive aggregation in the K^+-containing buffer, which might be due to a nonspecific monovalent cation effect.

Modulation of FtsZ Assembly by Temperature and Solution Variables—In order to learn how the assembly of FtsZ may be modulated, the effects of solution variables on the critical concentration were examined. The effect of temperature on FtsZ assembly induced by GMPCPP and Mg^{2+} at pH 6.5 is shown by Fig. 5*A*. No significant differences in electron micrographs of the polymers assembled at 30, 40, and 55 °C were observed. Control light scattering measurements with 0.1 mM GMPCPP and 1 mM GTP showed slower assembly, longer polymer stability periods and less scattering at the lower temperatures, particularly with GTP. The data in Fig. 5*A* were best fitted by a nonlinear integrated van't Hoff equation, from which the apparent values of the free energy ΔG^0_{app}, enthalpy ΔH^0_{app}, entropy ΔS^0_{app}, and the heat capacity change $\Delta C_{p,app}$, of the elongation reaction were calculated (see "Experimental Procedures"). The van't Hoff analysis predicts an optimal polymer stability, ΔG^0_{app} = −10.3 kcal mol^{-1}, at ~75 °C, close to the optimal growth temperature of *M. jannaschii* which is around 85 °C (41). The polymerization of FtsZ is characterized by an apparent change in heat capacity ΔC_p = −788 ± 105 cal K^{-1} mol^{-1}, it is endothermic and has a positive entropy change in the range of temperatures measured, 30–55 °C; the apparent enthalpic and entropic contributions to the free energy change are shown by Fig. 5*B*. The large negative heat capacity is compatible with the release of ordered water upon the formation of hydrophobic FtsZ-FtsZ contacts. Calculation of the change in apolar and polar accessible surface area (ΔASA) from the heat capacity change and the value of the enthalpy change (957 ± 500 cal mol^{-1} at 60 °C) by means of parametric structure-energetics relationships (42–44) results in ΔASA_{apolar} = −2050 ± 280 $Å^2$ and ΔASA_{pol} = −520 ± 310 $Å^2$, and it is compatible with a small change in conformational entropy (ca. −60 cal K^{-1} mol^{-1}) per FtsZ monomer added to the polymer.

The effects of magnesium, pH and ionic strength on the affinity of FtsZ polymer elongation with 0.1 mM GMPCPP were analyzed by sedimentation at 55 °C. Polymerization of FtsZ was not observed in the absence of added $MgCl_2$ (Cr > 30 μM

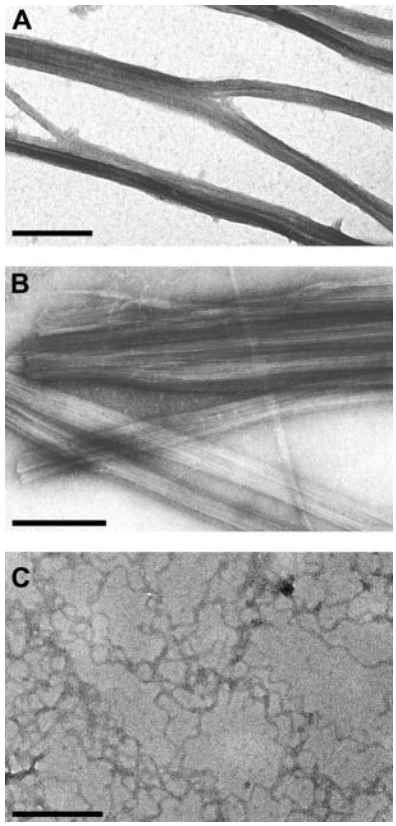

FIG. 4. **Electron micrographs of FtsZ polymers formed in potassium-containing Mes assembly buffer, pH 6.5, 10 mM $MgCl_2$, in the presence of 1 mM GTP (*A*), 0.1 mM GMPCPP (*B*), and in sodium-containing Mes assembly buffer, pH 6.5, 10 mM $MgCl_2$, in the presence 0.1 mM GMPCPP (*C*).** The FtsZ concentration was 12.5 μM. Bars are 200 nm.

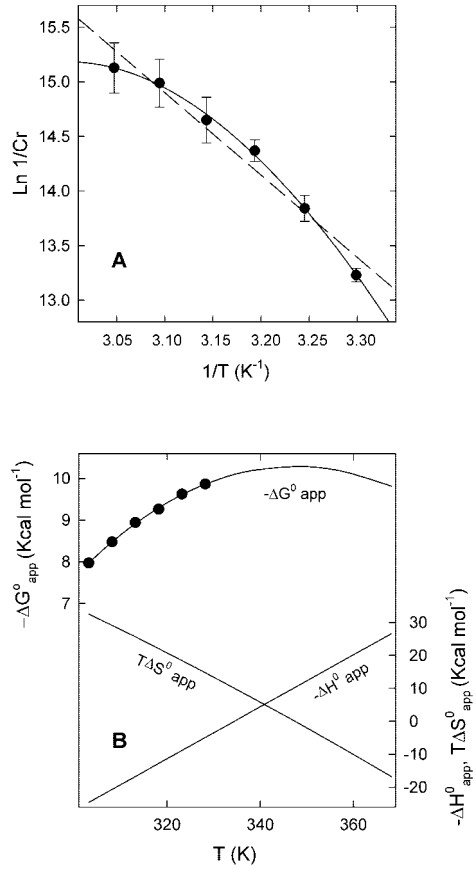

FIG. 5. *A*, Van't Hoff plot of FtsZ assembly in potassium-containing Mes assembly buffer, pH 6.5, with 10 mM $MgCl_2$ and 0.1 mM GMPCPP. The *solid line* is a non-linear van't Hoff fit, and the *dashed line* is a poorer linear van't Hoff fit shown for comparison. *B*, calculated enthalpy and entropy contributions to the apparent standard free energy change of FtsZ polymer elongation. The lines are the parameters resulting from the non-linear van't Hoff analysis (see "Experimental Procedures"; the fitting parameters were $a = 2714.42$, $b = -132485.63$, $c = -396.23$, from which the free energy, enthalpy, entropy changes can be calculated), and the points are the experimental free energy values. These lines are drawn beyond the experimentally accessible range simply to show the predicted behavior of the system at higher temperatures.

FtsZ; the residual free Mg^{2+} concentration in the EDTA-containing assembly buffer is ~10 nM). Adding Mg^{2+} resulted in assembly. The effects of Mg^{2+} activity on the elongation affinity were examined in terms of the linked functions theory (45). The Wyman linkage plot in Fig. 6*A* has a positive initial slope of 1.21 ± 0.15 between ~50 μM and ~300 μM free Mg^{2+}, which indicates the uptake of one magnesium ion per FtsZ molecule that is incorporated in the polymer, suggesting the participation in the assembly reaction of a Mg^{2+} ion with a medium apparent binding affinity. However, upon increasing the free Mg^{2+} concentration into the millimolar range, the slope becomes negative, −0.9 ± 0.15 (right side of the Wyman plot in Fig. 6*A*), which indicates the release of one low affinity magnesium ion per FtsZ molecule that is incorporated in the polymer, in the sense that one magnesium less is bound by the assembled FtsZ, but it does not establish a direct participation of these low affinity magnesium ions in polymerization. The effect of Mg^{2+}in the millimolar range on FtsZ polymerization has also been monitored by light scattering measurements, showing that when the concentration of $MgCl_2$ was increased, the polymerization and depolymerization turned slower, and the scattering increased suggesting polymer bundling, although no significant differences in their structure were observed by electron microscopy (not shown).

The effect of hydrogen ions is shown by Fig. 6*B*. FtsZ assembly is favored by lowering the pH. The elongation is more strongly pH-dependent in the range 6.0–7.2 than in the range 7.2–8.0; Pipes and Tris buffers appear to slightly weaken assembly with respect to phosphate and Mes buffers. Between pH 6.0 and 7.2 the slope of the Wyman plot is 0.64 ± 0.15, which indicates the uptake of less than one proton per FtsZ monomer incorporated in the polymer. Below pH 6.0 FtsZ started to precipitate (the calculated pI of FtsZ is 5.14), interfering with the assembly measurements. The formation of FtsZ polymers at different pH values (Pipes buffer, pH 6.5, 7.0, and 7.5; Mes buffer, pH 6.0 and 6.5; Tris buffer, pH 8.0) with 0.1 mM GMPCPP and 1 mM GTP was also followed by light scattering and electron microscopy. The light scattering was reduced with increasing pH and the filamentous polymers were thinner than those obtained at pH 6.5 (not shown). The effect of the ionic strength on FtsZ polymerization was tested sedimenting FtsZ at different KCl concentrations, in Mes buffer pH 6.5, 10 mM $MgCl_2$, 0.1 mM GMPCPP FtsZ, which showed that assembly is favored with increasing concentrations of KCl (the concentrations of KCl (M) and the corresponding critical concentration values of FtsZ (μM) were: 0 M, 0.73 ± 0.14 μM; 0.025 M, 0.47 ± 0.29 μM; 0.05 M, 0.30 ± 0.05 μM; 0.1 M, 0.26 ± 0.09 μM; 0.2 M, 0.18 ± 0.04 μM).

FtsZ Polymerization with Nucleoside Diphosphate—Sedimentation measurements initially intended as negative controls surprisingly indicated cooperative polymerization of FtsZ with GDP and GMPCP, provided enough protein concentration was reached. Fig. 7*A* compares the results with GDP, GMPCP, GTP, and GMPCPP at pH 6.0. Control measurements without Mg^{2+} gave negligible FtsZ sedimentation. The critical protein concentration values at pH 6.0 and 6.5 (with K^+ and Na^+) are

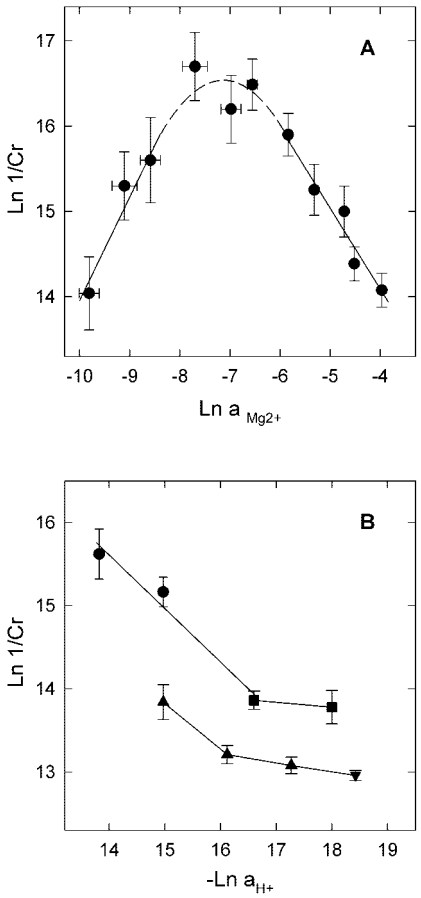

FIG. 6. *A*, Wyman plot of FtsZ polymer elongation with GMPCPP 0.1 mM at 55 °C as a function of the activity of magnesium ions in potassium-containing Mes assembly buffer, pH 6.5. The *solid lines* are linear fits in the low and high magnesium ion activity regions, and the *dashed line* has been drawn simply to show the trend of the data. *B*, Wyman plot of FtsZ polymer elongation with 0.1 mM GMPCPP and 10 mM $MgCl_2$ at 55 °C, as a function of the activity of hydrogen ions; the different buffers employed are: potassium-containing Mes assembly buffer, (●); 50 mM potassium phosphate, 50 mM KCl, 1 mM EDTA, (■); 50 mM PIPES, 50 mM KCl, 1 mM EDTA (▲); and 50 mM Tris, 50 mM KCl, 1 mM EDTA (▼).

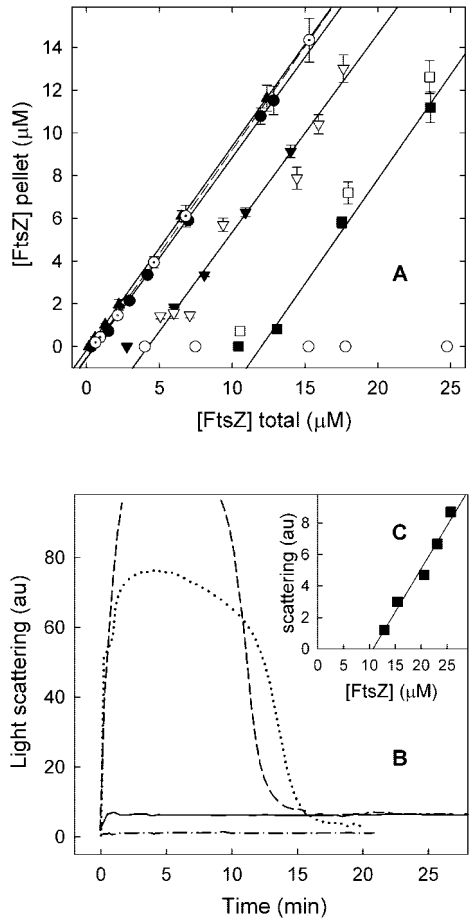

FIG. 7. *A*, FtsZ assembly measured by sedimentation in potassium-containing Mes assembly buffer, pH 6.0, 10 mM $MgCl_2$ at 55 °C, with 0.1 mM GMPCPP (▲), or 1 mM GTP (●), or 0.1 mM GMPCP (▼), or 1 mM GDP (■), or 1 mM GDP plus Ficoll 70 (200 g/liter) (☉ and *dashed line*), or 1 mM GDP without added $MgCl_2$ (○). FtsZ was also assembled with 0.1 mM GMPCPP (▽) or 1 mM GTP (□) which were let to hydrolyze before sedimentation. *B*, assembly of FtsZ monitored by light scattering in potassium-containing Mes assembly buffer pH 6.0, at 55 °C. Assembly was started by addition of 10 mM $MgCl_2$ and nucleotide as indicated. FtsZ (23 μM) assembly with 1 mM GDP (——), and with 1 mM GTP (- - -); FtsZ (13 μM) assembly with 1 mM GDP (-·-·-·) and with 1 mM GTP (·····). *Inset C*, Critical concentration plot of FtsZ assembly measured by light scattering in potassium assembly buffer pH 6.0, at 55 °C with 10 mM $MgCl_2$ and 1 mM GDP.

listed in Table I. The critical concentrations values for polymerization of GDP (GMPCP)-liganded FtsZ were about one order of magnitude larger than those of assembly with GTP (GMPCPP). FtsZ had been previously equilibrated with 10 μM GDP or GMPCP by gel chromatography, prior to polymerization with 1 mM GDP or 0.1 mM GMPCP respectively. The nucleotide bound to polymers assembled with GDP was 98% GDP (2% GTP); the nucleotide bound to polymers assembled with GMPCP was 80% GMPCP (20% GMPCPP) (Table I). The sedimentation measured with GDP (Fig. 7*A*) cannot be due to the 2% residual GTP-bound FtsZ, since (i) its concentration is below the critical concentration for assembly with GTP, (ii) most of the FtsZ in the solution was competent to assemble (instead of 2%), as shown by the unitary slope of the plot in Fig. 7*A*, and (iii) FtsZ polymers containing 100% GDP could be obtained when FtsZ in the supernatant of a polymerization with GDP was concentrated and polymerized again.

The polymerization of GDP-liganded FtsZ was also examined by light scattering. The light scattering of GDP-FtsZ polymers was ~15-fold smaller than with GTP (but much larger than the scattering of FtsZ oligomers without magnesium), suggesting the formation of thinner polymers, and it did not decay with time (Fig. 7*B*). In a reverse experiment, FtsZ was assembled with GTP and let to hydrolyze the nucleotide. The solution reached a similar scattering value as with GDP (Fig. 7*B*), and when it was centrifuged the pelleted FtsZ polymer contained 93% GDP and 7% GTP (supernatant: 100% GDP). Interestingly, these polymers, which had hydrolyzed the GTP had nearly the same critical concentration as the polymers directly assembled from GDP-bound FtsZ, and a similar result was obtained with GMPCPP and GMPCP (see Fig. 7*A*). In order to further confirm the FtsZ polymerization with GDP, the FtsZ condensation polymerization reaction was boosted by including 200 g/liter Ficoll 70 in the solution (47), which resulted in a reduction of the critical concentration to a value comparable to that of FtsZ-GTP in dilute buffer (Fig. 7*A*).

The polymers assembled from GDP-bound FtsZ with crowder were easily visualized by electron microscopy and had the appearance of helical ribbons 30–35 nm wide (Fig. 8, *A* and *B*); these were occasionally observed among a majority of straight filamentous polymers formed with GTP under the same crowded conditions (see Fig. 8*D*) and accumulated at longer times giving images similar to the polymers assembled with GDP. The FtsZ polymers formed with GMPCP and no crowder were a mixture of curly filaments (Fig. 8*C*) and large straight

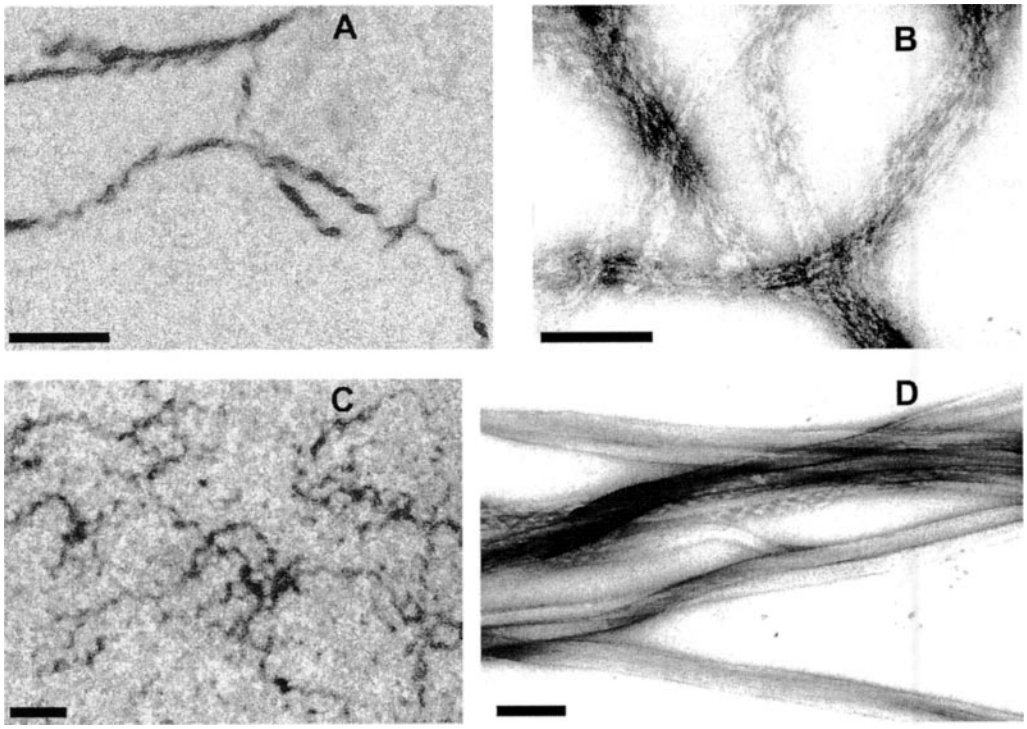

FIG. 8. **Electron micrographs of FtsZ assembly products with GDP and GMPCP in potassium-containing Mes assembly buffer, pH 6.0, 10 mM $MgCl_2$.** *A* and *B*, FtsZ (12.5 μM) with 1 mM GDP in the presence of Ficoll 70 (200 g/liter). *C*, FtsZ (20.6 μM) with 0.1 mM GMPCP. *D*, FtsZ (12.5 μM) with 1 mM GTP and Ficoll 70 (200 g/liter), shown for comparison. Bars are 200 nm.

polymers similar to those assembled GMPCPP (not shown, see Fig. 4*B*). We could not reproducibly visualize the GDP-FtsZ polymers without crowder by negative stain electron microscopy, which could be explained if they were more fragile thinner spiral filaments, which collapsed by adsorption onto the grid.

From these results we concluded that *M. jannaschii* FtsZ polymerization proceeds with nucleotide diphosphate forming different, helically curved polymers, whose elongation is weaker than the elongation of the straight polymers assembled with nucleotide triphosphate. The apparent increment free energy changes of polymer elongation $\Delta\Delta G^0_{g,app}$ (triphosphate − diphosphate) are listed in Table II. Assembly is similarly more favorable with GMPCPP compared with polymerization with GMPCP, and with GTP compared with GDP, by -2.03 ± 0.24 or -1.01 ± 0.14 kcal mol^{-1} (depending on the K^+- or Na^+-containing buffer employed), which are relatively small free energy changes.

DISCUSSION

FtsZ Assembly and Oligomerization—This work includes results clearly showing that reversible equilibrium assembly of purified FtsZ from the Archaea *M. jannaschii* is a cooperative process which takes place above a critical protein concentration, following a nucleated condensation polymerization mechanism (36), in dilute buffer near neutral pH. The GTP-induced assembly of FtsZ from bacteria was previously reported cooperative (16, 19, 22), or on the contrary to consist of the noncooperative isodesmic association of monomers into single-stranded filaments observed with scanning transmission electron microscopy (23). The nucleotide modulation of *E. coli* FtsZ assembly, known to give long polymers with GTP but shorter or no structures with GDP, is difficult to explain with a single protofilament, because it would require a very large affinity change of the only contact between monomers (23). Very recently, it has been argued that the assembly of single stranded filaments of FtsZ from *E. coli* is "apparently cooperative" (48). However, since cooperative assembly requires multiple contacts of each monomer in the polymer, a long filament made of a single row of monomers cannot conceivably assemble in a cooperative fashion (36). Cooperative assembly requires multiple-stranded polymers, and the formation of fiber polymers made of multiple filaments is typically cooperative. Cooperative polymers are typically long, whereas isodesmic filaments are typically short. FtsZ from *M. jannaschii* cooperatively assembles (Fig. 3) into multiple filament polymers and isolated filaments (Fig. 4), and each filament is probably made of two symmetrical tubulin-like protofilaments (26). We conclude that assembly of purified FtsZ is cooperative. In fact, the assembly of FtsZ from *E. coli* is cooperative under ionic microsolute and macromolecular crowding conditions resembling the bacterial cytosol (47). The degree of cooperativity (the ratio of the growth to the nucleation equilibrium constants; Ref. 36) and the size of the assembly nucleus remain to be investigated. The assembly kinetics of *E. coli* FtsZ is relatively fast, requiring stopped-flow methods (24), and no lag phase has been reported, suggesting assembly nuclei made of a few monomers.

The Mg^{2+}-induced oligomerization of GDP-FtsZ from *E. coli* has been extensively characterized by analytical ultracentrifugation in dilute buffer, and it is best fitted by an indefinite quasi-isodesmic linear self-association (24). This association was weakly modified by GTP. However, changing to a lower pH buffer and increasing temperature triggered a different reaction, consisting of the GTP-dependent assembly of FtsZ into long filaments. It was proposed that the linear oligomers correspond to segments of polymer protofilaments devoid of the additional GTP-promoted interactions of cooperative bidimensional assembly (see Fig. 1 and Scheme I in Ref. 24). In the case of FtsZ from *M. jannaschii,* a protein concentration-dependent oligomer formation has been observed, which is, however, insensitive to Mg^{2+} or the presence of a nucleotide γ-phosphate (Fig. 1 of this work). This association might have a functional relevance, such as the formation of the nucleus of a double-stranded filament, or be a side association reaction of FtsZ from *M. jannaschii*. Simply increasing the temperature of the Mg^{2+}-

TABLE II
Increment apparent free energy change of FtsZ polymer elongation induced by nucleotide γ phosphate

Free energy increment (kcal mol^{-1})	K^+-assembly buffer		Na^+-assembly buffer	
	pH 6.5	pH 6.0	pH 6.5	pH 6.0
$\Delta\Delta G^0_{app}$ (GMPCPP-GMPCP)	−2.35 ± 0.15	−2.13 ± 0.06	−1.10 ± 0.06	−0.89 ± 0.15
$\Delta\Delta G^0_{app}$ (GTP-GDP)	−1.69 ± 0.06	−1.98 ± 0.08	nd	−1.04 ± 0.12

containing FtsZ solution at sufficient protein concentration triggered cooperative assembly.

Thermodynamics of FtsZ Assembly in Comparison with Tubulin—The growth reaction of the FtsZ polymer proceeds with a sizeable negative apparent heat capacity change, and positive apparent enthalpy and entropy changes (Fig. 5), consistent with the burial of water-accessible hydrophobic surface areas, similarly to tubulin (37, 40, 49); such hydrophobic areas have been identified at the longitudinal contact interfaces of tubulin (6, 50). The optimal stability of the polymer of FtsZ from *M. jannaschii* is, however, displaced to a higher temperature closer to the optimal growth temperature of this thermophile. The changes in accessible surface area calculated from the data, $\Delta ASA_{apolar} = -2050 \pm 280$ Å^2 and $\Delta ASA_{pol} = -520 \pm 310$ Å^2 per FtsZ monomer added to the polymer, are nearly accounted for by the values calculated for the axial contact only in a tubulin-like FtsZ protofilament model (21, 25), $\Delta ASA_{apolar} = -1390$ Å^2 and $\Delta ASA_{pol} = -980$ Å^2 per monomer.

The assembly of FtsZ with GMPCPP proceeds at lower critical concentration than with GTP, as for tubulin (49, 51, 52). The effect of pH was also similar to tubulin (33), with the uptake of less than one H^+ ion per FtsZ assembled (Fig. 6*B*). Interestingly, minimal levels of Mg^{2+} activity are required for the assembly of FtsZ from *M. jannaschii* and one Mg^{2+} ion is incorporated per assembled FtsZ monomer (see "Results" and Fig. 6*A*), which relates to tubulin as follows. Both tubulin and FtsZ from *M. jannaschii* bind Mg^{2+} ions coordinated with the nucleotide at their top longitudinal association interfaces (34, 53–55). One high affinity bound Mg^{2+} ion at the nucleotide site of α-tubulin (at the dimerization interface), controls the stability of the tubulin dimer (34), whereas one medium affinity bound Mg^{2+} coordinated with the γ-phosphate of the exchangeable β-tubulin nucleotide (at the polymerization interface), functionally controls the microtubule polymer stability (34, 53, 54, 56). We suggest that the participation of a medium affinity Mg^{2+} ion in FtsZ polymer elongation (see "Results") entails the binding of this Mg^{2+} ion to the nucleotide site, similarly to the case of β-tubulin. On the other hand, the low apparent affinity Mg^{2+} ion released per FtsZ assembled (Fig. 6*A*, *right arm*) is an effect opposite to tubulin (33). Mg^{2+} is known to be required for GTP hydrolysis by FtsZ from different bacteria (19, 22, 57–59), and from *M. janaschii* (26), although FtsZ from *E. coli* was reported to assemble without Mg^{2+} (16, 60).

The Nucleotide γ-Phosphate Hydrolysis Switch and FtsZ Polymer Disassembly—Like other GTPases, the GDP-bound form of FtsZ from *M. jannaschii* is regarded as inactive, and it was not expected to polymerize (26). One unexpected finding of this study was the cooperative polymerization of GDP- and GMPCP-bound FtsZ, at high enough protein concentrations. The crystallographic structure of *M. jannaschii* FtsZ is known in the GDP bound form of the protein (Ref. 5; biochemically confirmed in Ref. 25), but a GTP-bound monomer or a high resolution polymer structure have not been reported. The potential structural changes of FtsZ activation by GTP were investigated by molecular dynamics simulations, in which the γ-phosphate of GTP consistently induced a conformational change of loop T3 (which is in a position equivalent to switch II of Ha-*ras*-p21) propagating to the hinge between the two segments of helix H3. A mutant FtsZ was constructed containing a single tryptophan instead of Thr-92 in loop T3, whose fluorescence was sensitive to having the GDP or GTP nucleotide bound 12 Å away, in support of the molecular dynamics results (25). Loop T3 is located at the contact interface between two FtsZ monomers in the model filament (21) and the change predicted to be induced in loop T3 upon GTP hydrolysis may bend the filament by pushing against helix H8 of next monomer, potentially explaining the disassembly of a straight multistranded polymer (25). As it is shown by the assembly results (exemplified by Fig. 7 and Table II), the activation of FtsZ for assembly by nucleotide triphosphate (GTP or GMPCPP) translates in a modest advantage of 1 or 2 kcal mol^{-1} (depending on solution conditions) for polymer elongation with nucleotide triphosphate over elongation with nucleotide diphosphate. This is suggestive of a flexibility change or a small structural change between the GTP and GDP-bound FtsZ states. It is possible that propagation of such change is what makes GDP-bound FtsZ polymerize into the abundant helical structures observed (Fig. 8, *A* and *B*) instead of the predominantly straight polymers formed with GTP (Fig. 8*D*). The fewer helical ribbons observed with GTP (Fig. 8*D*) are probably the result of nucleotide hydrolysis. We do not know whether the spontaneous polymerization of GDP-bound FtsZ is a property of the archaeal FtsZ investigated or might be shared by bacterial FtsZs under favorable solution conditions. Curved conformations with GDP were previously observed in FtsZ from *E. coli*, which formed minirings onto cationic phospholipid monolayers, but not in solution, and in helical FtsZ tubes formed with the polycation DEAE-dextran (20); it may be argued that complexation with these ionic additives can modify the polymer geometry. In our case, helical polymers of GDP-bound FtsZ have been observed with a non-ionic macromolecular crowder, which should not modify the polymer structure but by favoring the more compact forms.

In the case of tubulin, the GDP-liganded protein does not assemble into microtubules, but self-associates forming double rings (61). Pure GDP-tubulin was found unable to elongate microtubules, but it blocked microtubule ends (62). Tubulin rings are structurally equivalent to separated coiled protofilaments (63, 64), which are normally tensioned inside microtubules once GTP hydrolysis has taken place. It is tempting to speculate that the protofilament structure in helically polymerized GDP-bound FtsZ may correspond to the circular self-association of GDP-tubulin, with a modification of the twist angle between subunits, which makes difficult a planar curvature of GDP-FtsZ filaments. FtsZ polymers would helically curl in block prior to disassembly, at difference with the fraying protofilaments at depolymerizing microtubule ends. On the other hand, the difference between GDP- and GTP-liganded FtsZ may be regarded as a shift in the equilibrium between assembly-inactive and active states of the protein (61) in terms of linked equilibria (45), instead of an all or none activation switch.[4]

In the cytosol of *M. jannaschii*, the apparent affinity of FtsZ

[4] Assembly of tubulin with the GDP analogue GMPCP has been reported to proceed with critical concentration values that can be estimated to be two orders of magnitude larger than with GMPCPP under the same solution conditions (52, 49). Consequently, polymerization of GDP-tubulin might be expected to take place at practically unachievable concentrations of hundreds of mg per ml.

assembly should increase with temperature, by ~0.5 kcal/mol with respect to the value determined with purified FtsZ at 55 °C (Fig. 5), slightly increase with ionic strength (see "Results"), shift by pH (Fig. 6*B*) in an unknown direction, and increase by macromolecular crowding (Fig. 7*A*). The small value of the increment elongation affinity $\Delta\Delta G^0_{g,app}$ (GTP-GDP) should not be modified by macromolecular crowding (unless the nucleotide-induced structural change involved an unexpectedly large volume or shape change of FtsZ), and it is not modified by pH in the limited range examined (Table II). Let us assume for the purpose of this discussion that $\Delta\Delta G^0_{g,app}$ (GTP-GDP) is not largely altered by the temperature and the ionic composition of the archaeal cytosol. It might then be asked how the FtsZ-GDP polymer disassembly, which is believed necessary for its physiological dynamics during cell division, can proceed with such a small affinity difference. A simplistic answer would be by operating in a FtsZ concentration window centered at Cr (GTP) < [FtsZ] < Cr (GDP), in which FtsZ will assemble with GTP and fully disassemble with GDP (for an example, at 10 μM FtsZ under the conditions of Fig. 7). However, both Cr values (GDP and GTP) are expected to be considerably lower in the archaeal cytosol due to macromolecular crowding (see above), so that if the concentration of FtsZ is in the ~10 μM range (as in *E. coli*; Ref. 19), FtsZ would not spontaneously depolymerize upon GTP hydrolysis. Instead, it might form different GDP-containing polymers which may not be functionally active in the Z-ring, because they may be shorter helical instead of straight polymers, or may bend or be more fragile and fragment at the GDP-bound subunits. Additionally, disassembly of archaeal GDP-FtsZ may require inhibitory proteins, similar to bacterial MinC (65), SulA (66, 67), or EzrA (68).

Finally, this study has given thermodynamic insight into FtsZ assembly, but it does not address the dynamics of purified FtsZ polymers. The GTP hydrolysis switch of FtsZ should be the basic property for FtsZ polymer disassembly and its functional dynamics, however, the mechanisms need not be as in tubulin. A partially hydrolyzed nucleotide content in archaeal FtsZ polymers (Results), would argue against a microtubule-like GTP-cap/GDP-body treadmilling model for FtsZ polymers (near 100% GDP polymer, Ref. 69), but would favor either exchangeability of the nucleotide in the polymers (70) but perhaps at a limited rate (mixed polymers made of GTP- and GDP-bound subunits), or a transient assembly of GTP-FtsZ followed by disassembly of GDP-FtsZ polymers and nucleotide exchange in monomers (rapidly cycling polymers). Distinguishing between the mixed, rapidly cycling, or other polymers may require solution kinetic or single polymer biophysical studies.

Acknowledgments—We wish to thank M. A. Oliva for continued help, Drs. G. Rivas and J. F. Díaz for insightful discussions, Drs. J. M. Valpuesta, J. Bonkovic, and O. Llorca for advice and help with electron microscopy, Dr. J. M. Sanchez-Ruiz for calculations of accessible surface area, Drs. C. Alfonso and G. Rivas for the analytical ultracentrifugation analysis, and M. Alba for technical help.

REFERENCES

1. Shapiro, L., and Losick, R. (2000) *Cell* **100,** 89–98
2. Shapiro, L., McAdams, H. H., and Losick, R. (2002) *Science* **298,** 1942–1946
3. Alberts, B. (1998) *Cell* **92,** 291–294
4. Nogales, E., Wolf, S. G., and Downing, K. H. (1998) *Nature* **391,** 199–203
5. Lowe, J., and Amos, L. A. (1998) *Nature,* **391,** 202–206
6. Nogales, E., Whittaker, M., Milligan, R. A., and Downing, K. H. (1999) *Cell* **96,** 79–88
7. Kabsch, W., Mannherz, H. G., Suck, D., Pai, E. F., and Holmes, K. C. (1990) *Nature* **347,** 37–44
8. van den Ent, F., Amos, L. A., and Lowe, J. (2001) *Nature* **413,** 39–44
9. van den Ent, F., Moller-Jensen, J., Amos, L. A., Gerdes, K., and Lowe, J. (2002) *EMBO J.* **21,** 6935–6943
10. van den Ent, F., and Lowe, J. (2000) *EMBO J.* **19,** 5300–5307
11. Lutkenhaus, J. (2002) *Curr. Opin. Microbiol.* **5,** 548–552
12. Meinhardt, H., and de Boer, P. A. (2001) *Proc. Natl. Acad. Sci. U. S. A.* **98,** 14202–14207
13. Sun, Q., and Margolin, W. (1998) *J. Bacteriol.* **180,** 2050–2056
14. Stricker, J., Maddox, P., Salmon, E. D., and Erickson, H. P. (2002) *Proc. Natl. Acad. Sci. U. S. A.* **99,** 3171–3175
15. Mukherjee, A., and Lutkenhaus, J. (1994) *J. Bacteriol.* **176,** 2754–2758
16. Mukherjee, A., and Lutkenhaus, J. (1998) *EMBO J.* **17,** 462–469
17. Erickson, H. P., Taylor, D. W., Taylor, K. A., and Bramhill, D. (1996) *Proc. Natl. Acad. Sci. U. S. A.* **93,** 519–523
18. Yu, X. C., and Margolin, W. (1997) *EMBO J.* **16,** 5455–5463
19. Lu, C., Stricker, J., and Erickson, H. P. (1998) *Cell Motil. Cytoskel.* **40,** 71–86
20. Lu, C., Reedy, M., Erickson, H. P. (2000) *J. Bacteriol.* **182,** 164–170
21. Lowe, J., and Amos, L. A. (1999) *EMBO J.* **18,** 2364–2371
22. White, L., Ross, L. J., Reynolds, R. C., Seitz, L. E., Moore, G. D., and Borhani, D. W. (2000) *J. Bacteriol.* **182,** 4028–4034
23. Romberg, L., Simon, M., and Erickson, H. P. (2001) *J. Biol. Chem.* **276,** 11743–11753
24. Rivas, G., Lopez, A., Mingorance, J., Ferrandiz, M. J., Zorrilla, S., Minton, A. P., Vicente, M., and Andreu, J. M. (2000) *J. Biol. Chem.* **275,** 11740–11749
25. Diaz, J. F., Kralicek, A., Mingorance, J., Palacios, J. M., Vicente, M., and Andreu, J. M. (2001) *J. Biol. Chem.* **276,** 17307–17315
26. Oliva, M. A., Huecas, S., Palacios, J. M., Martin-Benito, J., Valpuesta, J. M., and Andreu, J. M. (2003) *J. Biol. Chem.* **278,** 33562–33570
27. Andreu, J. M., Oliva, M. A., and Monasterio, O. (2002) *J. Biol. Chem.* **277,** 43262–43270
28. Seckler, R., Wu, G. M., and Timasheff, S. N. (1990) *J. Biol. Chem.* **265,** 7655–7661
29. Perrone, P. A., and Brown, P. R. (1984) *J. Chromatogr.* **317,** 301–310
30. Minton, A. P. (1994) in *Modern Analytical Ultracentrifugation* (Schuster, T., and Laue, T., eds) pp. 81–93, Birkhauser Boston, Inc., Cambridge, MA
31. Philo, J. S. (1997) *Biophys. J.* **72,** 435–444
32. Bradford, M. (1976) *Anal. Biochem.* **72,** 248–254
33. Lee, J. C., and Timasheff, S. N. (1977) *Biochemistry* **16,** 1754–1764
34. Menéndez, M., Rivas, G., Díaz, J. F., and Andreu, J. M. (1998) *J. Biol. Chem.* **273,** 167–176
35. Oosawa, F., and Kasai, M. (1962) *J. Mol. Biol.* **4,** 10–21
36. Oosawa, F., and Asakura, S. (1975) *Thermodynamics of the Polymerization of Protein*, Academic Press, London
37. Lee, J. C., and Timasheff, S. N. (1975) *Biochemistry* **14,** 5183–5187
38. Andreu, J. M., and Timasheff, S. N. (1986) *Methods Enzymol.* **130,** 47–59
39. Erickson, H. P. (1989) *J. Mol. Biol.* **206,** 465–474
40. Díaz, J. F., Menéndez, M., and Andreu, J. M. (1993) *Biochemistry* **32,** 10067–10077
41. Jones, W. J., Leigh, J. A., Mayer, F., Woese, C. R., and Wolfe, R. S. (1983) *Arch. Microbiol.* **136,** 254–261
42. Luque, I., and Freire, E. (1998) *Methods Enzymol.* **295,** 100–128
43. Luque, I., Gómez, J., and Freire, E. (1998) *Proteins* **30,** 74–85
44. Spolar, R. S., and Record, M. Y., Jr. (1994) *Science* **263,** 777–789
45. Wyman, J., and Gill, S. (1990) *Binding and Linkage*, *Functional Chemistry of Biological Macromolecules*, University Science Books, Mill Valley, CA
46. Record, T. M., Courtenay, E. S., Cayley, S., and Gutman, H. J. (1998) *Trends Biochem. Sci.* **23,** 190–194
47. Gonzalez, J. M., Jimenez, M., Velez, M., Mingorance, J., Andreu, J. M., Vicente, M., and Rivas, G. (2003) *J. Biol. Chem.* **278,** 37664–37671
48. Caplan, M., and Erickson, H. P. (2003) *J. Biol. Chem.* **278,** 13784–13788
49. Vulevic, B., and Correia, J. J. (1997) *Biophys. J.* **72,** 1357–1375
50. Chacon, P., and Wriggers, W. (2002) *J. Mol. Biol.* **317,** 375–384
51. Hyman, A. A., Salser, S., Drechsel, D. N., Unwin, N., and Mitchison, T. J. (1992) *Mol. Biol. Cell* **3,** 1155–1167
52. Caplow, R. L., Ruhlen, R. L., and Shanks, J. (1994) *J. Cell Biol.* **127,** 779–788
53. Correia, J. J., Baty, L. T., and Williams, R. C. (1987) *J. Biol. Chem.* **262,** 17278–17284
54. Correia, J. J., Beth, A. H., and Williams, R. C. (1988) *J. Biol. Chem.* **263,** 10681–10686
55. Lowe, J., Li., H., Downing, K. H., and Nogales, E. (2001) *J. Mol. Biol.* **313,** 1045–1057
56. Carlier, M. F., Didry, D., and Valentin-Ranc, C. (1991) *J. Biol. Chem.* **266,** 12361–12368
57. de Boer, P., Crossley, R., and Rothfield, L. (1992) *Nature* **359,** 254–256
58. RayChaudhuri, D., and Park, J. T. (1992) *Nature* **359,** 251–254
59. Mukherjee, A., Dai, K., and Lutkenhaus, J. (1993) *Proc. Natl. Acad. Sci. U. S. A.* **90,** 1053–1057
60. Mukherjee, A., and Lutkenhaus, J. (1999) *J. Bacteriol.* **181,** 823–832
61. Howard, W. D., and Timasheff, S. N. (1986) *Biochemistry* **25,** 8292–8300
62. Carlier, M. F., Didry, D., and Pantaloni, D. (1987) *Biochemistry* **26,** 4428–4437
63. Diaz, J. F., Pantos, E., Bordas, J., Andreu, J. M. (1994) *J. Mol. Biol.* **238,** 214–225
64. Nogales, E., Wang, H. W., and Niederstrasser, H. (2003) *Curr. Opin. Struct. Biol.* **13,** 256–261
65. Pichoff, S., and Lutkenhaus, J. (2001) *J. Bacteriol.* **183,** 6630–6635
66. Justice, S. S., Garcia-Lara, J., and Rothfield, L. I. (2000) *Mol. Microbiol.* **37,** 410–423
67. Cordell, S., Robinson, E. J. H., and Löwe, J. (2003) *Proc. Natl. Acad. Sci. U. S. A.* **100,** 7889–7894
68. Levin, P. A., Kurtser, I. G., and Grossman, A. D. (1999) *Proc. Natl. Acad. Sci.* **96,** 9642–9647
69. Scheffers, D. J., and Driessen, A. J. M. (2002) *Mol. Microbiol.* **43,** 1517–1521
70. Mingorance, J., Rueda, S., Gomez-Puertas, P., Valencia, A., and Vicente, M. (2001) *Mol. Microbiol.* **41,** 83–91
71. Vicente, M., and Löwe, J. (2003) *EMBO Reports* **4,** 655–660
72. Jaenicke R., and Lilie, H. (2000) *Adv. Protein Chem.* **53,** 329–401
73. Scheffers, D., and Driessen, A. J. (2001) *FEBS Lett.* **506,** 6–10